

Solvent-free photo-thermocatalytic oxidation of benzyl alcohol on Pd/TiO₂(B) nanowires

Mingming Du^{a,*}, Ganning Zeng^{a,*}, Changhui Ye^a, Hao Jin^a, Jiale Huang^b, Daohua Sun^b, Qingbiao Li^b, Bing Chen^c, Xiaonian Li^{a,*}

^a College of Chemical Engineering, Zhejiang University of Technology, Hangzhou, 310014, PR China

^b Department of Chemical and Biochemical Engineering, College of Chemistry and Chemical Engineering, Xiamen University, Xiamen, 361005, PR China

^c Northern Region Persistent Organic Pollution Control (NRPOP) Laboratory, Engineering and Applied Science, Memorial University of Newfoundland, A1B1X5, St. John's, NL, Canada

ARTICLE INFO

Keywords:

TiO₂(B)
Pd
Photo-thermocatalysis
Benzyl alcohol
Solvent-free

ABSTRACT

TiO₂(B) is typical crystal structure for TiO₂, besides anatase, rutile and brookite. In this work, one-dimensional TiO₂(B) modified by Pd were prepared. The obtained Pd/TiO₂(B) was used for photo-thermocatalytic benzyl alcohol oxidation. Well-matched heterostructure contact boundary between (111) planes of Pd nanoparticles and (003) planes of TiO₂(B) was formed, which might facilitate interfacial photo-generated electrons transfer. The Pd/TiO₂(B) catalyst exhibited enhanced the photo-thermocatalytic activity, attributed to the synergistic effect of Pd, TiO₂(B) and their well-matched heterojunction, and also the synergism between the thermocatalysis and photocatalysis.

1. Introduction

Photocatalytic benzyl alcohol (BzOH) oxidation over semiconductors materials [1–4], such as TiO₂ [5–8], CeO₂ [9,10], Bi₄O₅Br₂ [11], C₃N₄ [12], H₂Ti₃O₇ [13] and CdS [1] semiconductors, is one of efficient method to produce benzaldehyde (BzH). Especially, TiO₂ semiconductor has received a lot of attention among the semiconductors materials [14–16], due to its high photocatalytic performance and stability [17–21], which is strongly depended on its crystal structure [5]. Such as, Li, et al. found high BzH selectivity can be obtained over rutile TiO₂ under visible-light irradiation [22]. Brookite TiO₂ gave 56 % selectivity of aldehyde, 3 times higher than that with anatase/rutile mixed phases [23]. Besides, brookite, anatase and rutile, TiO₂(B) is also typical crystallographic forms of TiO₂, which was discovered by Marchand et al. [24]. TiO₂(B) as photocatalysts has wide applications in photodegradation of methyl orange [25], photocatalytic hydrogen production [26] and so on [27].

Usually, high photocatalytic performance of BzOH oxidation over TiO₂ was only obtained under the solvent of acetonitrile [7,28], toluene [6], H₂O [29] or trifluorotoluene [3]. Actually, it is more environmentally friendly for BzOH oxidation under the solvent-free condition, avoiding toxic and harmful solvents. However, there is very poor photocatalytic activity over bare TiO₂ under the solvent-free condition.

Only 0.2 % of BzOH conversion was obtained for TiO₂(P25) under the solvent-free condition at 60 °C [30]. Although, the TiO₂ was modified by metal nanoparticles, such as Au, Ag, Pd, Pt, Rh or Ir, the BzOH conversion still lower than 10 % at 6 h under 250 W Hg lamp [30].

TiO₂ nanowires with special physical and chemical properties have advantages as photocatalysts, which supported on the graphene oxide exhibited much higher photodegradation activity for methylene blue in comparison with TiO₂ nanoparticles [31]. In this work, 1D TiO₂(B) nanowires supporting Pd nanoparticles were prepared, and were used for solvent-free photo-thermocatalytic oxidation of BzOH with atmospheric O₂. Pd/TiO₂(B) nanowire catalyst shows high photo-thermocatalytic activity and stability in BzOH oxidation to produce BzH, due to the synergistic effect among Pd, TiO₂(B) and their well-matched heterojunction.

2. Experimental section

2.1. Materials

Chemical reagents (P25, HCl, NaOH) : Sinopharm Chemical Reagent. Palladium Nitrate and *C. Platycladi* leaves (CP) : Adamas Reagent Co. Ltd and Xiamen Jiuding Drugstore, respectively.

* Corresponding authors.

E-mail addresses: dumingming2008@126.com (M. Du), g nzeng@zjut.edu.cn (G. Zeng), xnli@zjut.edu.cn (X. Li).

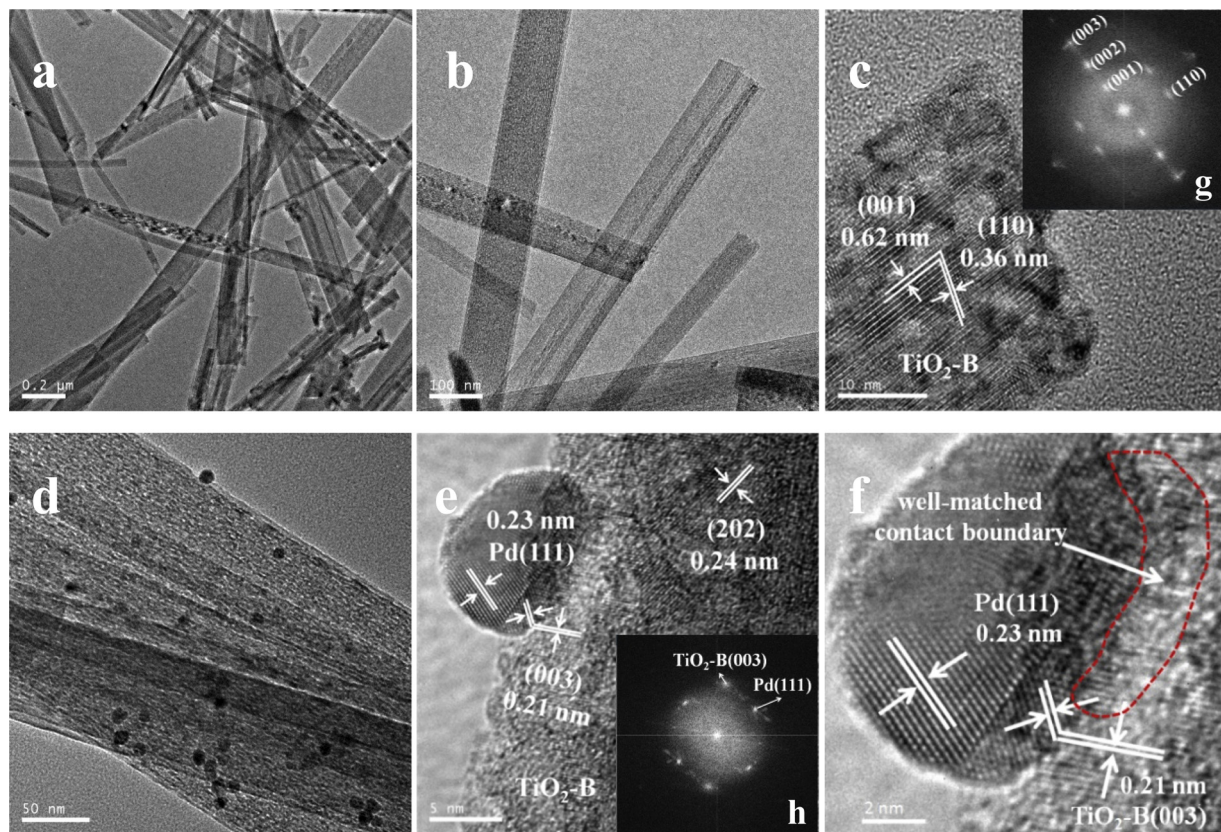


Fig. 1. TEM and corresponding FFT images for $\text{TiO}_2(\text{B})$ and $\text{Pd}/\text{TiO}_2(\text{B})$; a-c: TEM and HRTEM images of $\text{TiO}_2(\text{B})$, g: FFT image of $\text{TiO}_2(\text{B})$, d-e: TEM images of $\text{Pd}/\text{TiO}_2(\text{B})$ nanowires, f: HRTEM of $\text{Pd}/\text{TiO}_2(\text{B})$ nanowires, h: FFT image of $\text{Pd}/\text{TiO}_2(\text{B})$ nanowires.

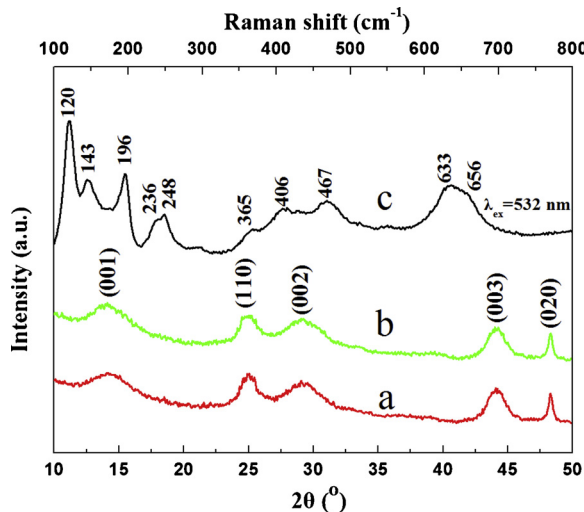


Fig. 2. XRD (a: $\text{TiO}_2(\text{B})$, b: $\text{Pd}/\text{TiO}_2(\text{B})$) and Visible Raman (c: $\text{TiO}_2(\text{B})$) spectra of the samples.

2.2. Synthesis of $\text{TiO}_2(\text{B})$ nanowries

$\text{TiO}_2(\text{P}25)$ was dispersed in NaOH aqueous solution, then transferred into a teflon-lined autoclave container for 48 h at 200°C . $\text{TiO}_2(\text{B})$ nanowires were obtained after washed by deionized water and HCl , dried and calcinated at 300°C .

2.3. Synthesis of $\text{Pd}/\text{TiO}_2(\text{B})$ catalysts

The $\text{Pd}/\text{TiO}_2(\text{B})$ catalyst was prepared by SI method [32–36]. 10 g/L

CP extract was prepared by our previous study [32,33]. Firstly, Pd sol were prepared by mixing $\text{Pd}(\text{NO}_3)_2$ (74 mM) and CP extract at 90°C . Then Pd nanoparticles were supported onto $\text{TiO}_2(\text{B})$ nanowires by mixing Pd sol and $\text{TiO}_2(\text{B})$ to obtain the $\text{Pd}/\text{TiO}_2(\text{B})$ nanowires catalysts.

2.4. Characterization of the catalysts

The surface area: Tristar 3000; Crystal Structure: XRD, X'Pert Pro X-ray diffractometer; Light absorption property: DRUV-vis, varian cary-5000 spectrometer; Morphology: TEM, Tecnai F30 microscope; Actual Pd loadings and chemical nature were obtained by AAS and XPS, respectively.

2.5. Catalytic activity measurements

Solvent-free photo-thermocatalytic benzyl alcohol oxidation using O_2 was carried out in quartz flask at 90°C . The light source was halogen lamp(150 W). 0.1 g catalyst and 10 mL benzyl alcohol was mixed with oxygen of 90 mL/min. Gas chromatography was used to analyze the resulting product.

3. Results and discussion

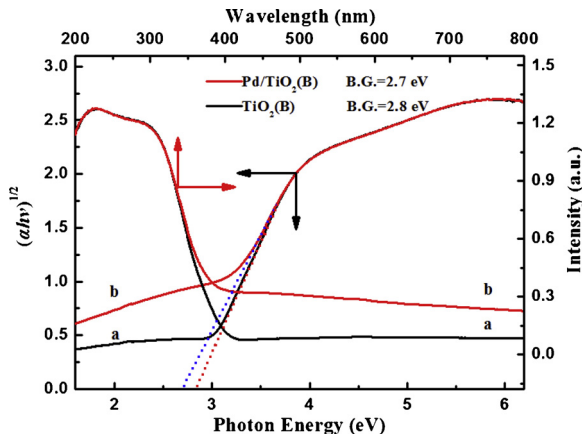
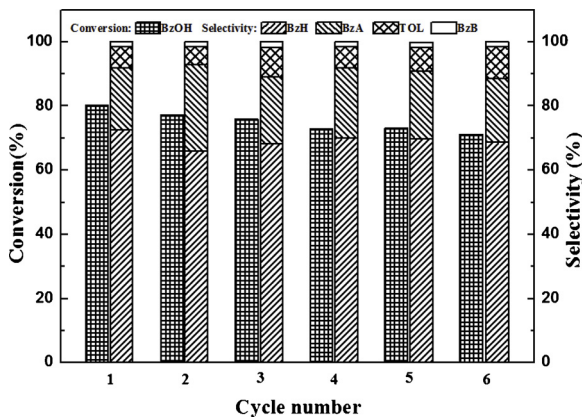
3.1. Characterizations of the catalyst

$\text{TiO}_2(\text{B})$ were prepared by hydrothermal synthesis method [25,37], and The $\text{Pd}/\text{TiO}_2(\text{B})$ nanowires catalysts were prepared by sol-immobilization method [32,33]. As shown in Fig. 1, the obtained sample is 1D TiO_2 nanowire in Fig. 1(a and b), and the lattice spacings of the crystal planes were approximately 0.36 and 0.62 nm, which corresponds to that of the (110) and (001) crystal planes from $\text{TiO}_2(\text{B})$

Table 1Catalytic performance for BzOH oxidation by Pd/TiO₂(B) catalyst.

Catalysts	T (°C)	Light	T (h)	Con. (%)	Sel. (%)				Yield (%)	TOF ^a (h ⁻¹)	BzH productivity (mol kg _{cat.} ⁻¹ h ⁻¹)
					BzH	BzA	TOL	BzB			
Pd/TiO ₂ (B)	90	Light	2	55.6	70.3	2.4	25.4	2.1	39.1	2735	180
			4	81.9	69.7	17.4	10.2	2.7	57.1	2016	132
Pd/TiO ₂ (B)	90	NO	2	39.5	72.9	1.9	24.3	0.9	28.8	1944	133
Pd/TiO ₂ (B)	30	Light	4	2.7	89.7	5.6	3.7	1.0	2.4	66	6
TiO ₂ (B)	90	Light	4	2.0	79.3	8.7	0.0	12.0	1.6	50	4
NO	90	Light	4	1.9	92.1	4.6	0.9	3.4	1.7	47	4
Pd/TiO ₂ (P25)	90	Light	6	68.8	73.8	22.5	1.9	1.8	50.8	1128	78

BzA: Benzoic acid, BzB: Benzyl benzoate, TOL: Toluene.

^a Moles of converted BzOH per mole of metal per hour.Fig. 3. DRUV-Vis spectra and Kubelka-Munk transformed spectra of TiO₂(B) and Pd/TiO₂(B).Fig. 4. Catalytic performance of the recycled Pd/TiO₂(B)nanowires catalyst.

nanowire (Fig. 1c). TiO₂(B) crystal planes were also confirmed by FFT (Fig. 1g). There are typical (001), (002), (003) and (110) crystal planes of TiO₂(B). As shown in Fig. 1(d and e), Pd NPs were highly dispersed on the TiO₂(B) nanowire in Fig. 1(d). We also found that the well-matched heterostructure contact boundary between (111)planes of Pd NPs and (003) planes of TiO₂(B) was obviously seen in the HRTEM images in Fig. 1(e and f) [37–39]. The Fourier transformation patterns also display the typical (111) crystal plane of Pd NPs and (003) crystal plane of TiO₂(B) nanowire of Pd/TiO₂(B) catalyst in Fig. 1(h).

Crystal phase structure of TiO₂(B) was also characterized using XRD and visible Raman spectroscopy. As shown in Fig. 2(a), the diffraction peaks at $2\theta = 14.19^\circ$, 24.93° , 28.61° , 43.51° and 48.53° are reflections from the (001), (110) and (002) et al. planes of the TiO₂(B) (Ref. code: 46–1237). There is no change for those diffraction peaks associated

with TiO₂(B) after loading Pd NPs in Fig. 2(b). However, no Pd NPs peak was observed, indicating that Pd NPs might be well dispersed on TiO₂(B) nanowire. Raman spectroscopy excited by 532 nm laser of the TiO₂(B) nanowire is displayed in Fig. 2(c), the typical bands of TiO₂(B) phase appear at 120, 143, 196 cm⁻¹ appear [40], consistent with XRD, visible Raman spectroscopy and HRTEM results.

Pd²⁺ ions can be reduced to Pd⁰ species for the Pd/TiO₂(B) catalyst, which has been demonstrated by the result of the XPS [41], the detail analysis can be seen in Fig. S2 and Table S1. The detail information of BET surface area, pore diameter and pore volume can also be seen in Fig. S1.

3.2. Photocatalytic activity measurements

The photo-thermocatalytic activity of the obtained catalysts was shown in Table 1. Without light irradiation, Pd/TiO₂(B) nanowires only gave 39.5 % of BzOH conversion at 90 °C after 2 h. Under light irradiation, the Pd/TiO₂(B) nanowire gave higher catalytic activity with 55.6 % of BzOH conversion, 70.3 % of BzH selectivity and TOF of 2735 h⁻¹ at 90 °C after 2 h. Only 68.8 % of conversion was obtained for Pd/TiO₂(P25) at 6 h, which is much lower than that of Pd/TiO₂(B) nanowire catalyst even at 4 h (81.9 % of BzOH conversion). Almost no photocatalytic performance for Pd/TiO₂(B) nanowires at 30 °C, suggesting that there is a synergism between thermocatalysis and photocatalysis [19].

As shown in Fig. 3, Pd/TiO₂(B) nanowires showed enhanced light adsorption, compared with bare TiO₂(B). Therefore, more electrons (e^-) and holes (h^+) pair can be produced, according to the photo-thermocatalytic reaction mechanism⁷. The e^- can be transferred along the axial direction of TiO₂(B) nanowire to Pd NPs through the well-matched heterostructure contact boundary between (111)planes of Pd NPs and (003) planes of TiO₂(B) nanowires. Therefore, more e^- and h^+ were separated efficiently. The holes react with α -C–H of BzOH to give BzOH radicals⁷. The photo-induced electrons can promote Pd sites to active oxygen molecules, yielding O_2^- . It can cleave OH– bond of benzyl alcohol radical, forming BzH⁶. Without Pd NPs, oxygen molecules activation was decreased [42–44], therefore, bare TiO₂(B) gave only 1.9 % of BzOH conversion. Therefore, synergistic effect among Pd, TiO₂(B) and their well-matched heterojunction played an important role photocatalytic synthesis of BzH.

The Pd/TiO₂(B) nanowires catalyst also present high catalytic stability. There is no obviously decrease for BzOH conversion after six recycle utilization (Fig. 4). Compared with the catalytic performance from the previous studies, as shown in Table S2, the obtained Pd/TiO₂(B) nanowires catalyst present high catalytic activity, especially, High BzH yield and TOF are simultaneously achieved.

4. Conclusions

In summary, Pd/TiO₂(B) nanowires for photo-thermocatalytic BzOH

oxidation was prepared. Well-matched heterojunction from (111) planes of Pd NPs and (003) planes of TiO₂(B) was formed, which facilitate photo-generated e⁻ transfer. Aslo, the Pd/TiO₂(B) showed enhanced light adsorption. Therefore, the catalyst exhibited enhanced photo-thermocatalytic performance which is mainly due to the synergistic effect among the Pd, TiO₂(B) and the contact boundary.

Author contributions

M. Du and G. Zeng designed the project.

M. Du wrote the manuscript.

M. Du, G. Zeng, C. Ye and H. Jin performed the experiments and analyzed the results. J. Huang, D. Sun, Q. Li, X. Li and B. Chen provided useful suggestions to this work.

Declaration of Competing Interest

The authors declare that they have no known competing financial interests or personal relationships that could be perceived as influencing the work reported in this paper.

Acknowledgements

This work is supported by National Nature Science Foundation (21606198 and 51728902), Zhejiang province Natural Science Foundation (LY20B060008, LGF18D060002 and LQ18G030018).

Appendix A. Supplementary data

Supplementary material related to this article can be found, in the online version, at doi:<https://doi.org/10.1016/j.mcat.2020.110771>.

References

- [1] Y. Liu, P. Zhang, B. Tian, J. Zhang, ACS Appl. Mater. Inter. 7 (2015) 13849–13858.
- [2] C. Meng, K. Yang, X. Fu, R. Yuan, ACS Catal. 5 (2015) 3760–3766.
- [3] Y. Chen, Y. Wang, W. Li, Q. Yang, Q. Hou, L. Wei, L. Liu, F. Huang, M. Ju, Appl. Catal. B-Environ. 210 (2017) 352–367.
- [4] D. Spasiano, L.D.P. Rodriguez, J.C. Olleros, S. Malato, R. Marotta, R. Andreozzi, Appl. Catal. B-Environ. 136 (2013) 56–63.
- [5] S. Yurdakal, G. Palmisano, V. Loddio, V. Augugliaro, L. Palmisano, J. Am. Chem. Soc. 130 (2008) 1568–1569.
- [6] T. Jiang, C. Jia, L. Zhang, S. He, Y. Sang, H. Li, Y. Li, X. Xu, H. Liu, Nanoscale 7 (2015) 209–217.
- [7] S. Higashimoto, N. Suetsugu, M. Azuma, H. Ohue, Y. Sakata, J. Catal. 274 (2010) 76–83.
- [8] S. Higashimoto, K. Okada, T. Morisugi, M. Azuma, H. Ohue, T.H. Kim, M. Matsuoka, M. Anpo, Top. Catal. 53 (2010) 578–583.
- [9] A. Tanaka, K. Hashimoto, H. Kominami, J. Am. Chem. Soc. 134 (2012) 14526–14533.
- [10] B.X. Li, B.S. Zhang, S.B. Nie, L.Z. Shao, L.Y. Hu, J. Catal. 348 (2017) 256–264.
- [11] C. Zheng, G. He, X. Xiao, M. Lu, H. Zhong, X. Zuo, J. Nan, Appl. Catal. B-Environ. 205 (2017) 201–210.
- [12] P. Zhang, J. Deng, J. Mao, H. Li, Y. Wang, Chinese J. Catal. 36 (2015) 1580–1586.
- [13] M. Du, G. Zeng, J. Huang, D. Sun, Q. Li, G. Wang, X. Li, ACS Sustain. Chem. Eng. (2019).
- [14] L.J. Han, B.T. Su, G. Liu, Z. Ma, X.C. An, Mol. Catal. 456 (2018) 96–101.
- [15] X.X. Zhao, Y. Zhang, P. Wen, G. Xu, D. Ma, P. Qiu, Mol. Catal. 452 (2018) 175–183.
- [16] R. Fiorenza, M. Bellar, J. Mol. Catal. A-Chem. 415 (2016) 56–64.
- [17] M. Cheng, S. Yang, R. Chen, X. Zhu, Q. Liao, Y. Huang, Mol. Catal. 448 (2018) 185–194.
- [18] M. Zeng, Y. Li, M. Mao, J. Bai, L. Ren, X. Zhao, ACS Catal. 5 (2015) 3278–3286.
- [19] C. Ren, L. Zhou, Y. Duan, Y. Chen, J. Rare Earth 30 (2012) 1106–1111.
- [20] L. Palmisano, E.I. Garcia-Lopez, G. Marci, Dalton Trans. 45 (2016) 11596–11605.
- [21] A. Golabiewska, W. Lisowski, M. Jarek, G. Nowaczky, M. Michalska, S. Jurga, A. Zaleska-Medynska, Mol. Catal. 442 (2017) 154–163.
- [22] C.-J. Li, G.-R. Xu, B. Zhang, J.R. Gong, Appl. Catal. B-Environ. 115 (2012) 201–208.
- [23] M. Addamo, V. Augugliaro, M. Bellardita, A. Di Paola, V. Loddio, G. Palmisano, L. Palmisano, S. Yurdakal, Catal. Lett. 126 (2008) 58–62.
- [24] R. Marchand, L. Brohan, M. Tournoux, Mater. Res. Bull. 15 (1980) 1129–1133.
- [25] W. Zhou, L. Gai, P. Hu, J. Cui, X. Liu, D. Wang, G. Li, H. Jiang, D. Liu, H. Liu, J. Wang, CrystEngComm 13 (2011) 6643–6649.
- [26] F.L. Wang, Y.J. Jiang, A. Gautam, Y.R. Li, R. Amal, ACS Catal. 4 (2014) 1451–1457.
- [27] W. Zhuang, L.H. Liu, W. Li, R. An, X. Feng, X.B. Wu, Y.D. Zhu, X.H. Lu, Chinese J. Chem. Eng. 23 (2015) 583–589.
- [28] S. Higashimoto, R. Shirai, Y. Osano, M. Azuma, H. Ohue, Y. Sakata, H. Kobayashi, J. Catal. 311 (2014) 137–143.
- [29] Z.Z. Zhang, Z.S. Luo, Z.P. Yang, S.Y. Zhang, Y. Zhang, Y.G. Zhou, X.X. Wang, X.Z. Fu, RSC Adv. 3 (2013) 7215–7218.
- [30] W. Feng, G. Wu, L. Li, N. Guan, Green Chem. 13 (2011) 3265–3272.
- [31] X. Pan, Y. Zhao, S. Liu, C.L. Korzeniewski, S. Wang, Z.Y. Fan, ACS Appl. Mater. Inter. 4 (2012) 3944–3950.
- [32] Y. Zhou, W. Lin, H. Wang, Q. Li, J. Huang, M. Du, L. Lin, Y. Gao, L. Lin, N. He, Langmuir 27 (2011) 166–169.
- [33] F. Lu, D. Sun, J. Huang, M. Du, F. Yang, H. Chen, Y. Hong, Q. Li, ACS Sustain. Chem. Eng. 2 (2014) 1212–1218.
- [34] M. Du, J. Huang, D. Sun, D. Wang, Q. Li, Ind. Eng. Chem. Res. 57 (2018) 14910–14914.
- [35] M. Du, D. Sun, H. Yang, J. Huang, X. Jing, T. Odoom-Wubah, H. Wang, L. Jia, Q. Li, J. Phys. Chem. C 118 (2014) 19150–19157.
- [36] T. Odoom-Wubah, Q. Li, Q. Wang, M.Z.R. Usha, J.L. Huang, Q.B. Li, Mol. Catal. 469 (2019) 118–130.
- [37] L. Qin, X. Pan, L. Wang, X. Sun, G. Zhang, X. Guo, Appl. Catal. B-Environ. 150 (2014) 544–553.
- [38] P. Zhang, Y. Gong, H. Li, Z. Chen, Y. Wang, Nat. Commun. 4 (2013) 1593.
- [39] Y. Cao, S. Mao, M. Li, Y. Chen, Y. Wang, ACS Catal. 7 (2017) 8090–8112.
- [40] J. Zhang, M.J. Li, Z.C. Feng, J. Chen, C. Li, J. Phys. Chem. B 110 (2006) 927–935.
- [41] T. Odoom-Wubah, Q. Li, I. Adilov, J.L. Huang, Q.B. Li, Mol. Catal. 477 (2019).
- [42] S. Aditya, C.T.C. E, S.J. E, W. Di, P. Laura, V. Alberto, Chemcatchem 9 (2017) 253–257.
- [43] S. Aditya, R. Ilenia, C.T.C. E, P. Laura, V. Alberto, Chemcatchem 8 (2016) 2482–2491.
- [44] S. Aditya, C.T.C. E, R. Ilenia, V. Alberto, P. Laura, Chemcatchem 6 (2014) 3464–3473.